# High-Q X-band and K-band Micromachined Spiral Inductors for Use in Si-based Integrated Circuits

Liang-Hung Lu, George E. Ponchak[+], Pallab Bhattacharya and Linda P. B. Katehi

Department of Electrical Engineering and Computer Science
University of Michigan, Ann Arbor, MI 48109-2122

[+]NASA Lewis Research Center, Cleveland, OH 44135

## ABSTRACT

A micromachined structure with reduced parasitics is proposed to enhance the resonant frequency and the quality factor (Q) of a spiral inductor. Inductors with various etch depths have been fabricated on a high resistivity Si substrate. Two-port S-parameters are measured to characterize the performance of the inductors. With an etch depth of 20 μm, a fabricated 1.8 nH spiral inductor achieves a maximum resonant frequency of 25.6 GHz and a maximum Q of 20.2 at 14.5 GHz. This technology is compatible with SiGe/Si HBT technology, and the spiral inductors are especially suitable for Si-based monolithic microwave integrated circuit (MMIC) applications.

## INTRODUCTION

With the advances in epitaxy technology, Si-based MMICs have been realized by incorporating SiGe/Si HBTs with mature Si technology. It is obvious that Si-based MMICs provide a promising solution to meet the need of the fast-growing market for wireless communication. However, the availability of high performance passive components, especially spiral inductors, plays an important role in circuit implementation. Limiting factors such as the Q-factor, resonant frequency and distributed effects of a spiral inductor have to be carefully investigated in microwave frequencies to allow for successful circuit design. Recently, efforts have been reported to improve the characteristics of a spiral inductor by using stacking metal layer [1], suspended structure [2] and patterned ground shields [3]. However, most demonstration of the proposed approaches have been focused at frequencies well below X-band.

In this work, micromachined spiral inductors have been proposed and characterized to demonstrate improved Q-factor and increased resonant frequency. Due to the compatibility of the technology, the proposed structure can be easily integrated into the existing Si-based MMIC process to meet the circuit demands up to K-band applications.

## DESIGN AND FABRICATION

For a rectangular spiral inductor, the design parameters include number of turns (N), inner/outer diameter (Di/Do), line width (W) and line spacing (S). The geometry parameters used in this work are fixed constant to 10 μm width, 10 μm spacing and a inner diameter of 50 μm for all inductor structures.

A spiral inductor is typically analyzed as a two-port network and it can be modeled by the equivalent circuit shown in Fig. 1(a), where L is the inductance and $R_s$ is the series resistance due to conductor losses and dissipation from the induced eddy currents in the substrate. $R_{Si}$ is the resistance of the Si substrate, and the shunt parasitic capacitances for silicon substrate, inter-metal dielectric and metal pads are presented by $C_{Si}$, $C_{ox}$ and $C_s$, respectively. To minimize the substrate loss, a high-resistivity Si substrate was chosen for the fabrication, thus minimizing the losses due to the finite substrate resistance $R_{Si}$ and eddy currents. A

0-7803-6255-1/00/$10.00 (c) 2000 IEEE

simplified equivalent circuit for the spiral inductor is shown in Fig. 1(b). To investigate the microwave characteristics, the inductor is characterized by a simplified equivalent circuit, Fig. 1(b), and is analyzed as an one-port network by grounding the second port. From the equivalent circuit, the admittance matrix parameter $1/Y_{11}$ is given by

$$\frac{1}{Y_{11}} = \frac{R_s}{(1-\omega^2 LC)^2 + \omega^2 R_s^2 C^2} + j\omega \frac{L(1-\omega^2 LC) - R_s^2 C^2}{(1-\omega^2 LC)^2 + \omega^2 R_s^2 C^2} \quad (1)$$

where $C=C_o+C_{p1}$. The spiral structure of Fig. 1(b) can be used as an inductor only for frequencies below the structure resonant frequency, which can be obtained analytically by zeroing the imaginary part of $Z_{11}$. Equation (1) indicates that the higher the inductance, the lower the resonant frequency. Due to low resonant frequencies, the application of these spiral inductors has to be limited. Another important issue needs to be considered in circuit design is the Q-factor. The definition of the quality factor Q is given by

$$Q = \frac{Im\left(\frac{1}{Y_{11}}\right)}{Re\left(\frac{1}{Y_{11}}\right)} = \frac{\omega L}{R_s} - \frac{\omega^2 LC}{R_s} - \omega R_s C \quad (2)$$

At lower frequencies, the quality factor can be approximated by $\omega L/R_s$, and its value first increases with frequency. However, the second and third terms in Equation (2) dominate at higher frequencies and cause Q to decrease with increasing frequency. Thus, a maximum Q ($Q_{max}$) is reached at $f_{Qmax}$. Since the roll-off of the Q-factor is caused by higher frequency parasitics, one effective technique to improve Q and increase resonant frequency is to minimize the parasitic capacitances $C_o$ and $C_p$. For a planar structure such as the spiral inductor, the effective permittivity ($\varepsilon_{r\text{-}eff}$) is approximated by $(1+\varepsilon_{r\text{-}substrate})/2$. By removing the substrate material in between the lines, $\varepsilon_{r\text{-}eff}$ is reduced. As a result, spiral inductors with enhanced Q and high resonant frequency can be achieved due to the reduction of parasitic capacitances.

The fabrication of the spiral inductor studied herein starts with a high resistivity Si substrate with a resistance of 2000 Ω-cm. A PECVD oxide layer with a thickness of 0.3 μm is deposited as the isolation layer between the substrate and the first metal layer (M1), which is used as underpass contact to return the inner terminal of the coil to the outside. The spiral loops are formed by the second metal layer (M2) with an 1 μm inter-metal dielectric in between these two metal layers. Both M1 and M2 are evaporated Al layers with thickness of

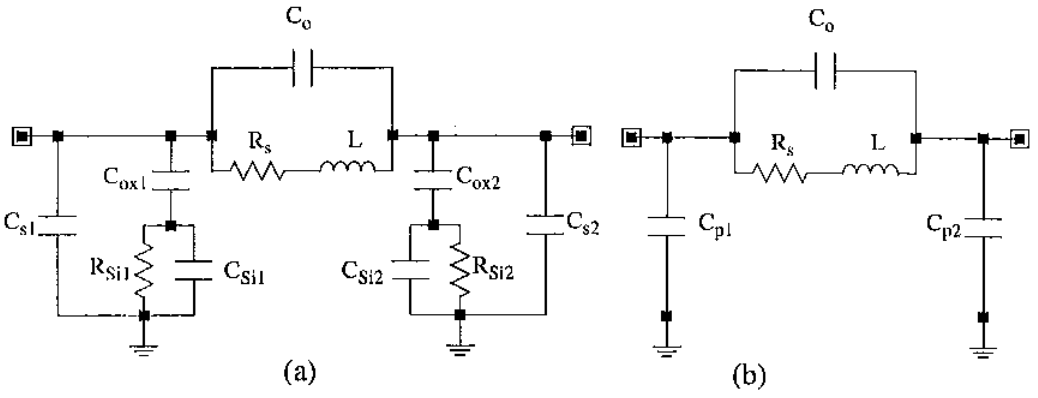


Fig. 1 (a) The equivalent circuit of the spiral inductor with a coplanar ground pad and (b) Simplified equivalent circuit of the spiral inductor on high-resistivity Si substrate.

1 μm and 3 μm, respectively. At this point, standard CMOS processing steps have been used to fabricate the inductors. To apply the micromachined structure to the spiral inductor, the metal layers are covered by a 0.1-μm-thick Ni layer which is then used as self-aligned etch mask. Finally, a deep trench created by RIE using $SF_6$ and $O_2$ completes the fabrication process. Figure 2 shows the photomicrograph of the fabricated spiral inductor with a micromachined structure.

## RESULTS AND DISCUSSION

On-wafer probing for two-port S-parameter measurement of the fabricated inductors is performed using HP8510C network analyzer. The frequency range covered by this measurement is from 2 GHz to 40 GHz. To eliminate the parasitics caused by the coplanar pad, the open-circuited pad is also measured and these results are used to de-embed [4] the measured S-parameters for the inductors. Following this step, the inductors are characterized by the one-port input impedance $Z_{11}$ calculated from de-embedded two-port measurement. The Q-factor is determined by the ratio of the imaginary part to the real part of $Z_{11}$, and the resonant frequency is chosen at the frequency which the imaginary part of $Z_{11}$ is crossing the zero point.

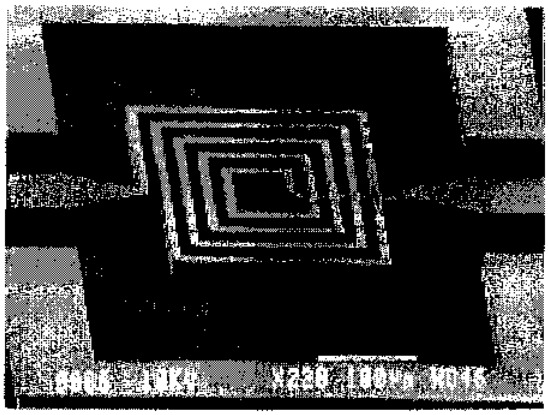

Fig. 2 The photomicrograph of the spiral inductor with a micromachined structure.

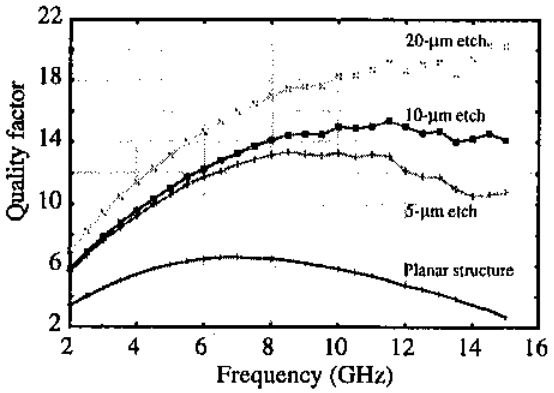


Fig. 3 Quality factor of the 3.5 turn spiral inductor with various etch depth.

To investigate the effect of this micromachined technology, inductor samples with etch depth of 0, 5, 10 and 20 μm, respectively, are prepared. For a spiral inductor with a turn number of 3.5, a 20 μm-deep etch increases the resonant frequency from 18.5 GHz to 25.6 GHz, and the maximum Q of 20.2 is observed at 14.5 GHz. The Q-factor of this inductor with various etch depth is shown in Fig. 3, and it is clear that both $Q_{max}$ and $f_{Qmax}$ increase as the etch depth increases. Based on the equivalent circuit shown in Fig. 1(b), the model parameters are extracted by fitting the equivalent circuits to the measured S-parameters using HP-EEsof LIBRA. From the extracted model parameters, it is obvious that the inductance L and series resistance $R_s$ are almost independent of the etch depth, however, the capacitances are reduced significantly due to the reduction of the effective permittivity by the deep etch. Since the etch was performed not only in between the loops but also in the area between the spiral lines and the coplanar ground, both $C_o$ and $C_p$ reduce substantially.

More extensive study has been done for the inductors with different geometry, and the performance of this technology is concluded in Table 1. As indicated by the measurement, the deeper the etch, the higher the resonant frequency and the better quality factor. However,

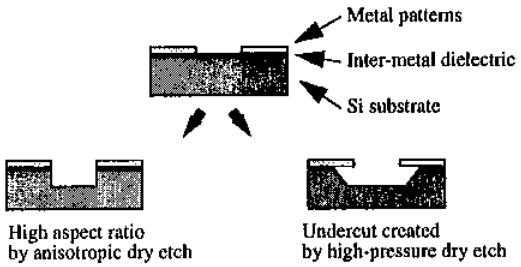


Fig. 4 Etch profile for the micromachined structure.

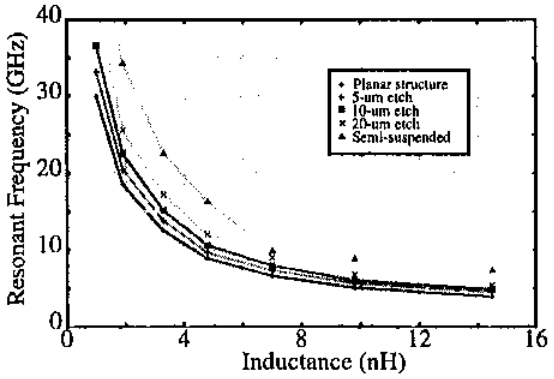


Fig. 5 Resonant frequencies of the spiral inductor with various etch depth.

comparing with the planar spiral inductors, an abrupt increase of Q factor is observed even for the inductors with 5 μm etch. It is believed that the etch not only reduces the parasitic capacitance, but also removes the conducting adhesion layer in the inter-metal dielectric.

Moreover, with a well-calibrated etch profile, an undercut can be introduced during the dry etch to further remove the substrate material as shown in Fig. 4, resulting in a semi-suspended micromachined structure. In this case, an effective permittivity similar to the suspended structure can be achieved while the spiral structure are still supported by the substrate for better mechanical stability. Fig. 5 shows the further increase of the resonant frequency in the semi-suspended structure.

## CONCLUSION

A novel Si micromachined inductive structure is proposed that is characterized by enhanced resonant frequency and the Q factor. In this technology, etched depth adds one more design parameter to the spiral inductor that

| Etch Depth | # of turns | 8.5 | 7.5 | 6.5 | 5.5 | 4.5 | 3.5 | 2.5 | 1.5 |
|---|---|---|---|---|---|---|---|---|---|
| | Inductance (nH) | 14.7 | 10.7 | 7.6 | 5.0 | 3.2 | 1.9 | 1.1 | 0.5 |
| 0 μm | $Q_{max}/f_{Qmax}$ (GHz) | - | 5.5/ 2 | 5.7/ 2.5 | 6/ 3 | 6.3/ 5.5 | 6.6/ 6.5 | 7.6/ 12.6 | - |
| | $f_{res}$ (GHz) | 4.0 | 5.5 | 7.1 | 9.5 | 13.5 | 18.5 | 30.0 | >40 |
| 5 μm | $Q_{max}/f_{Qmax}$ (GHz) | 10/ 2 | 11.1/ 3 | 11.7/ 3 | 12.6/ 4 | 13/ 6.5 | 13.4/ 9.6 | 16.6/ 18.7 | - |
| | $f_{res}$ (GHz) | 4.8 | 6.0 | 7.5 | 10.5 | 15.2 | 20.4 | 33.2 | >40 |
| 10 μm | $Q_{max}/f_{Qmax}$ (GHz) | 10.6/ 2 | 11.5/ 3 | 12.8/ 3.5 | 13.6/ 5.5 | 13.3/ 6.5 | 15.4/ 11.5 | 20.7/ 22 | - |
| | $f_{res}$ (GHz) | 5.2 | 6.5 | 8.5 | 11.5 | 16.9 | 22.5 | 36.6 | >40 |
| 20 μm | $Q_{max}/f_{Qmax}$ (GHz) | 12.8/ 3 | 14.3/ 3 | 13.8/ 4 | 16/ 6 | 13.6/ 9.5 | 20.2/ 14 | 31/ 23 | - |
| | $f_{res}$ (GHz) | 5.7 | 7.5 | 9.7 | 13.5 | 20.1 | 25.6 | >40 | >40 |

Table 1 Q and the resonant frequencies of the spiral inductors.

allows one to meet circuit requirements. Inductors with various turn numbers have been fabricated on a high resistivity substrate and characterized from 2 GHz to 40 GHz. As the resonant frequency and quality factor increase significantly by this technology, a low-loss lumped design can be realized up to Ku or even K-band. Since the process is compatible with SiGe/Si HBT technology, the micromachined spiral inductors can be integrated with active devices for Si-base MMIC applications.

## ACKNOWLEDGEMENT

This work is being supported by JPL under contraction 961358.

## REFERENCES

[1] Seung Won Peak and Kwang Seok Seo, "Air-Gap Stacked Spiral Inductor," IEEE Microwave and Guided Wave Letters, Vol. 7, No. 10, pp. 329-331, October 1997.

[2] J.Y.-C. Chang, Asad A. Abidi, and Micheal Gaitan, "Large Suspended Inductors on Silicon and Their Use in a 2-μm CMOS RF Amplifier", IEEE Electron Device Letters, Vol. 14, No. 5, pp. 246-248, May 1993.

[3] C. Patrick Yue, and S. Simon Wong, "On-Chip Spiral Inductors with Patterned Ground Shields for Si-Based RF IC's," IEEE Journal of Solid-State Circuits, Vol. 33, No.5, pp. 743-751, May 1998.

[4] P. J. van Wijnen, H. R. Claessen, and E. A. Wolsheimer, "A new straightforward calibration and correction procedure for 'on-wafer' high-frequency S-parameter measurements (45 MHz-18 GHz)," IEEE Bipolar Circuits and Technol. Meet., 1987, pp 70-73.